Enhanced terahertz sensitivity for glucose detection with a hydrogel platform embedded with Au nanoparticles

JINGJING ZHAO,[1,5] SHAOHUA LU,[1,5] JULIO BASTOS-ARRIETA,[2,3] CRISTINA PALET,[4] YILING SUN,[1] RENHENG WANG,[1] ZHENGFANG QIAN,[1] AND SHUTING FAN[1,*]

[1] *Key Laboratory of Optoelectronic Devices and Systems of Ministry of Education and Guangdong Province, College of Physics and Optoelectronic Engineering, Shenzhen University, 518060, China*
[2] *Department of Chemical Engineering and Analytical Chemistry, University of Barcelona, Martí i Franquès 1-11, 08028 Barcelona, Spain*
[3] *Institut de Recerca de l'Aigua (IdRA), University of Barcelona, 08028 Barcelona, Spain*
[4] *Group of Separation Techniques in Chemistry, Department of Chemistry, Universitat Autònoma de Barcelona, 08193 Bellaterra, Catalunya, Spain*
[5] *Contributed equally to this work*
[*]shutingfan@szu.edu.cn

Abstract: We presented a strategy for enhancing the sensitivity of terahertz glucose sensing with a hydrogel platform pre-embedded with Au nanoparticles. Physiological-level glucose solutions ranging from 0 to 0.8 mg/mL were measured and the extracted absorption coefficients can be clearly distinguished compared to traditional terahertz time domain spectroscopy performed directly on aqueous solutions. Further, Isotherm models were applied to successfully describe the relationship between the absorption coefficient and the glucose concentration ($R^2 = 0.9977$). Finally, the origin of the sensitivity enhancement was investigated and verified to be the pH change induced by the catalysis of Au nanoparticles to glucose oxidation.

1. Introduction

It has been reported that approximately 488 million people worldwide are suffering from diabetes in 2019 [1]. For diabetic patients, constant monitoring is a necessity to maintain their glucose level within a normal range. Currently, this has been realized with cost-efficient glucose biosensors based on electrochemical approaches [2–4]. However, most commercially available electrochemical biosensors use enzyme-modified electrodes which are lack of long-term stability (such as more than one month) due to the inevitably degradation of enzymes. In consequence, the development of a non-enzymatic technique for the reliable and sensitive detection of glucose is urgently desirable. Nanostructured noble metals, as an alternative to enzymes, have been successfully applied to the electrochemical sensing of glucose with a satisfactory limit of detection (LOD) [5–7]. Among them, gold nano particles (AuNPs) stand out as a suitable catalyst due to their ability to facilitate the glucose oxidation process without creating issues such as protein adsorption or having toxic effect at physiological pH [8–10]. Moreover, Au possesses glucose-oxidase-like (GOD) properties with high selective and sensitivity, and glucose detection based on AuNPs have been fabricated for commercial products [11].

Typically, a drop of blood by pricking fingers is required for the above electrochemical measurements which makes it painful for patients with a need of frequent blood sugar monitoring. Mini invasive devices measuring interstitial glucose levels are designed and applied in commercial products, however, real-time blood glucose monitoring can reflect the current condition of patients more accurately [11]. In fact, non-contact, non-invasive and continuous glucose sensing is more

easily realized with optical spectroscopic approaches at ultra-violet (UV) [12], visible, near-infrared (NIR) as well as mid-infrared (MIR) frequencies [13,14], and with technologies including Raman [15], fluorescence [16,17] and optical coherence tomography (OCT) [18]. However, there are many challenges remained in the before-mentioned optical methods. For examples, light in the MIR band suffers from a poor penetration depth through skin (only a few microns) [19], making it not suitable for non-invasive in vivo measurements. Raman spectroscopy, with excitation lasers operating at visible or NIR wavelengths, can induce background fluorescence in tissue, which will decrease the signal to noise ratio (SNR) from Raman scattering [20]. Regarding the fluorescence method, a labeling species is needed which can exhibit a photobleaching effect resulting in short lifetimes of the sensors [21].

Apart from the above well-studied optical wavelengths, terahertz (THz) waves, located in a less explored band in the electromagnetic (EM) spectrum, has received heated research discussions in the recent few decades. The term "terahertz" typically refers to EM waves in the 3.3-330 cm^{-1} (30–3000 μm) range. The photon energy at 1 THz is approximately 4.13 meV. Therefore, it is non-ionizing and featured with low-energy vibrational modes associated with weak intermolecular interactions such as hydrogen bonds. Compared to optical bands with much shorter wavelengths, the mechanism of interactions with biological tissues in the terahertz band is mainly absorption rather than scattering. The penetration depth in tissue of a nano-watt terahertz pulsed system with a 90 dB SNR can be hundreds of microns [22,23], making it a potential candidate for non-invasive, continuous, and subcutaneous/implantable glucose sensing. Furthermore, terahertz wave is not only a non-contact biosensing method, but also a carrier band for future-generation communication systems. Exploration of biosensing at terahertz frequencies will pave the way for future wireless communication/sensing integrated devices. Several attempts have been made to measure glucose in aqueous solutions with terahertz waves, but the sensitivity has not reached physiological levels yet, because of the large absorption by the hydrogen-bonded network of water. The sensitivity can be improved with metamaterials functioning at terahertz frequencies [24,25], but the fabrication process is tedious, and the supporting substrate limit their flexibility to be used in implantable devices. Recently, Zhou *et al.* have reported using hydrogel as a container for aqueous solutions [26]. They introduced the boronic acid when preparing the hydrogel to increase the selectivity for glucose. Their proposed methods can probe the aqueous glucose with a concentration of 0.2 mg/mL, thus providing a platform for various aqueous solutions probed by THz spectroscopy.

Here, we propose a strategy for terahertz glucose sensing with enhanced sensitivities using a hydrogel platform which is pre-embedded with AuNPs. The AuNPs function as catalysts to facilitate the oxidation of glucose to gluconic acid. When the glucose molecules are oxidized, the resulting pH change is correlated with the glucose concentration which can be picked up by terahertz waves [27,28]. Further, the hydrogel platform can largely prohibit the THz absorption caused by bulk water. Compared with the measurements directly performed on glucose aqueous solutions, the sensitivity of terahertz absorption measurements can be therefore greatly enhanced. Moreover, nano-diamonds (NDs) were used as a supporting material for AuNPs that have been synthesized following our previous work [29], as NDs can provide large adsorption sites for glucose leading to preconcentrated glucose on ND surface [30].

In this work, we first investigated the sensitivity enhancement effect of the proposed sensing strategy, and then correlated the THz absorption coefficient with the concentration of glucose solutions using isotherm models. Finally, we verified the origin of the sensitivity enhancement induced by pH change of the system. Overall, this work describes a promising approach for the non-enzymatic, non-labeling, continuous detection of glucose based on THz spectroscopy.

2. Experimental

2.1. Sample fabrication and characterization

2.1.1. Chemicals

Nano-diamonds (>87%), silver nitrate (≥99.0%), α-D-glucose (96%), sodium borohydride, and gold(III) chloride trihydrate were purchased from Aladdin (Shanghai, China). Sodium hydroxide (95%), acrylamide (AM), methylene-Bis-Acrylamide (BIS), ammonium persulphate (APS), phosphate buffered saline (PBS, 10 mmol/L, pH 8.0), phosphate buffered saline (PBS, 0.2 M, pH 7.4), glucose oxidase and ethanol (99%) were obtained from Macklin Reagent Co., Ltd. (Shanghai, China). Nitride acid (con.) was obtained from Fisher (Guangzhou, China zeyuan). All chemicals were of analytical grade and used without further purification.

2.1.2. Fabrication of the hydrogel with Au encapsulated inside

The functionalization of ND@Au was carried out following an intermatrix synthesis approach reported in our previous work [29]. ND@Au hydrogels were prepared following the literature with some modifications [31]. Firstly, three stock solutions were prepared by mixing 0.43 g of AM, 0.0204 g of BIS, and 0.25 g of APS in a 1.5 mL centrifuge tube. They were then dissolved in 1 mL of PBS solution (10 mM, pH 8.0) to a final concentration of 6.1 mol/L, 0.13 mol/L, and 1.1 mol/L for AM, BIS and APS, respectively. 250 mL of AM stock solution and 50 mL of BIS stock solution were first mixed in a vortex oscillator for 2 min, followed by the addition of 1.0 mg of Au and 50 mL of APS stock solution for another 2 min. After that, 15 μL of the mixed solution was dropped in the square mold with a dimension of 0.5 cm×0.5 cm×0.25 mm. The samples were later covered with coverslips and transferred to the oven at 60 °C for 30 min. APS was used as a cross linker to initiate the reaction. Finally, the synthesized hydrogels were removed from the mold by tweezers and kept in a sealed microcentrifuge tube for further study.

2.1.3. Material characterization

The morphology, structure, and physicochemical characteristics of NDs and ND@Au were characterized after fabrication. The particle powders were dissolved in ethanol (99%) in a 1.5 mL centrifuge tube and ultrasonicated for 5 min. After that, the dispersed solution was dropped onto a copper screen for further study. Transmission electron microscopy (TEM) (FEI Titan Cubed Themis G2 300, Holland), Scanning electron microscopy (SEM) (FEI Scios DualBeam FIB/SEM) were performed at Shenzhen University.

2.2. Apparatus and principles

2.2.1. Terahertz measurements

The THz measurements were carried out using a commercial terahertz time-domain spectroscopy (THz-TDS) system, TeraPulse 4000 (TeraView Ltd., Cambridge, UK), in transmission geometry. The details of the system can be found elsewhere [32]. The samples were measured in a chamber which was purged with high purity Nitrogen gas to remove the water vapor lines in the spectra. All the measurements were performed at 21°C (±1°C) with a relative humidity below 4%.

Figure 1 shows the protocol for THz-TDS measurements. A demountable liquid cell (PIKE Technologies Inc., USA) was used as a sample holder for the hydrogel measurements. The hydrogel samples were sandwiched between a pair of polyethylene windows with a 100 μm Teflon spacer. A separate measurement was made without the hydrogel and the spacer as a reference. Each sample was averaged from 300 waveforms. The absorption coefficient of the samples can then be extracted with the equations described in [33,34].

In this study, six hydrogels containing 1.0 mg of ND@Au nanoparticles were synthesized. 10 μ L of glucose solution with concentrations ranging from 0 to 0.8 mg/mL were dropped
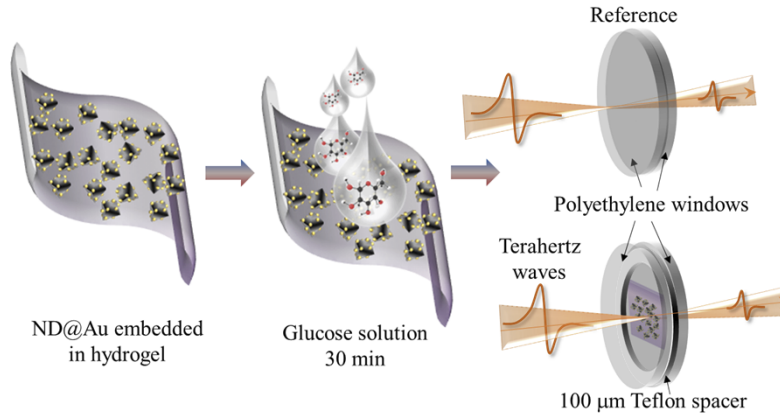
Fig. 1. Schematic drawing demonstrating the protocol for THz-TDS transmission measurement.

into each of the six freshly prepared AuNP hydrogels. Terahertz measurements of the hydrogel samples were performed after 30 min to make sure that all the glucose solutions have been completely absorbed by the hydrogels and allow enough reaction time for the glucose molecules to be fully oxidized to gluconic acid. For comparison, measurements are also performed directly on glucose solutions with the same concentrations with the same measurement setup. To validate the proposed absorption enhancement mechanism (pH change) of our sensing platform, we also prepared ND@Au solutions mixed with different concentrations of glucose. The pH values of the solutions were measured by a pH meter (Leici PHS-25, Shanghai) at reaction times of 0, 1 min and 30 min.

2.2.2.   Absorption coefficient of the hydrogel and the adsorption isotherm models

Soaked with the glucose solution, the hydrogel sensing platform can be considered as a composite material whose absorption coefficient α_{eff} follows a simple mixing rule as Eq. (1), where α_i is the THz absorption coefficient and ϕ_i is the volume fraction of ith component:

$$\alpha_{eff} = \sum_{i=1}^{n} \alpha_i \phi_i \tag{1}$$

Glucose molecules in the solution will diffuse into the hydrogel and be adsorbed onto the surface of Au nanoparticles. Sequentially, glucose oxidation catalyzed by AuNPs will take place following a two-step reaction: glucose is oxidized to gluconic acid after dehydrogenation, while O_2 can be reduced to H_2O_2 by two electrons, as shown in Eq. (2).

$$C_6H_{12}O_6(s) + O_2(g) + H_2O(l) \xrightarrow{Catalyst} C_6H_{12}O_7(l) + H_2O_2(l). \tag{2}$$
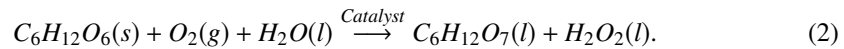
After 30 minutes, the system consisting of the nanoparticle-embedded hydrogel and the glucose solution will have reached an equilibrium. Considering that an equal amount of gluconic acid and H_2O_2 will be produced in this process, the absorption coefficient of the system can be expressed with Eq. (3):

$$\alpha_{eff} = \alpha_0 \cdot \left(1 - \phi_{GA} - \frac{v_{H_2O_2}}{v_{GA}} \cdot \phi_{GA}\right) + \alpha_{GA} \cdot \phi_{GA} + \alpha_{H_2O_2} \cdot \frac{v_{H_2O_2}}{v_{GA}} \phi_{GA} \tag{3}$$

where α_0, α_{GA}, and $\alpha_{H_2O_2}$ are the absorption coefficient of the hydrated hydrogel, gluconic acid, and H_2O_2, respectively; ϕ_{GA} is the volume fraction of the gluconic acid; v_{GA}=111.2 cm^3/mol and

$v_{H_2O_2}$=23.5 cm^3/mol are the molar volumes of gluconic acid and H$_2$O$_2$, respectively [35]. In the terahertz frequency range, α_{GA} and $\alpha_{H_2O_2}$ are both much smaller than the α_0 of the hydrated hydrogel. Therefore, α_{eff} can be further simplified as Eq. (4):

$$\alpha_{eff} = \alpha_0 - \alpha_0 \cdot (1 + \frac{v_{H_2O_2}}{v_{GA}}) \cdot \phi_{GA}. \tag{4}$$

As the glucose oxidation only happens for glucose molecules adsorbed on the surface of Au nanoparticles, ϕ_{GA} is equal to ϕ_g, which represents the volume fraction of glucose molecules adsorbed onto Au nanoparticles. To account for the change of the THz absorption coefficient with the glucose concentration, $\Delta\alpha_{eff}$ is defined with Eq. (5):

$$\Delta\alpha_{eff} = \alpha_{eff} - \alpha_0 = -\alpha_0 \cdot (1 + \frac{v_{H_2O_2}}{v_{GA}}) \cdot \phi_g. \tag{5}$$

Under a stable temperature, the thermodynamic system formed by the hydrogel and glucose solutions can be described with isotherm models, such as the Langmuir and Freundlich models. The former assumes that the uptake of glucose molecules occurs on homogeneous surfaces by a monolayer deposition, while the latter describes the equilibrium process on heterogeneous surfaces. The relationship between the fraction of the adsorbed glucose ϕ_g and the concentration of glucose in the solution C_g for the two models can be found in Eq. (6) and (7) [36,37]. In these equations, K_L is the Langmuir constant and ϕ_{gmax} denotes the maximum adsorption capacity, while K_F and n are the Freundlich constants:

$$\phi_g = \phi_{g\,max} \cdot \frac{K_L C_g}{1 + K_L C_g} \tag{6}$$

$$\phi_g = K_F C_g^n. \tag{7}$$

Finally, the concentration dependent change of the effective absorption coefficient for the equilibrium system can be modelled by substituting Eq. (6) or (7) into Eq. (5) for Langmuir and Freundlich models, respectively.

3. Results and discussions

3.1. Characterization of ND@Au

The structures of ND@Au were further investigated by TEM, as shown in Fig. 2(a)-(c). As can be seen from Fig. 2(a), EDS mapping of ND@Au confirms the presence of Au attached to the NDs. Furthermore, AuNPs are evenly distributed on the surface of ND, although aggregated as indicated by the red circle in Fig. 2(b), their average diameters are less than 50 nm. Moreover, the magnified TEM images in Fig. 2(c) showed that the diameters of the AuNPs were approximately 10 nm. Characterization of the ND@Au in hydrogels was performed by SEM as shown in Fig. 2(d) and the result clearly shows that the ND@Au particles are agglomerated to a primary size of around 200 nm, but they are evenly distributed in the hydrogels which is beneficial for the oxidization of glucose. The swelling rate (S) were checked to determine the water adsorption time by hydrogel, the hydrogel can reach adsorption saturation in 30 min. Thus, 30 min was chosen as the reaction time [38].

3.2. Glucose detection with terahertz waves on the hydrogel platform

First, glucose solutions (0-0.8 mg/mL) were directly measured in a liquid cell with a thickness of 100 µm. The absorption coefficients of the solutions are shown in Fig. 3(a), in which each curve is an average of three separate measurements. Subsequently, glucose solutions with the same concentrations were measured using our AuNP-embedded hydrogel platform. For each hydrogel,
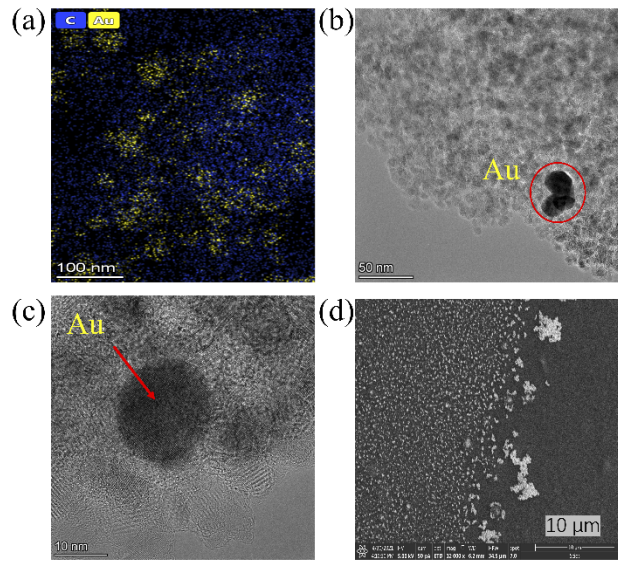
Fig. 2. (a) The EDS mapping image of ND@Au; (b) and (c) are the TEM images of ND@Au taken at different magnifications; (d) is the SEM image of ND@Au.

10 μL of the glucose solution was dropped onto the platform and allowed for 30 min reaction time. The frequency-dependent absorption coefficients of the samples are shown in Fig. 3(b). The absorption coefficient possesses a monotonic increasing trend with frequency over 0.2 to 1.5 THz for both sets of measurements in Fig. 3(a) and (b), which is mainly caused by the water content. Compared with the measurements directly performed on liquid solutions, the absorption coefficients measured with the hydrogel platform are clearly distinguished for different glucose concentrations. Considering that the normal physiological blood sugar level is between 0.7 to 1 mg/mL, this result demonstrates that our ND@Au-embedded hydrogel platform is promising for measuring glucose concentration at physiological level.
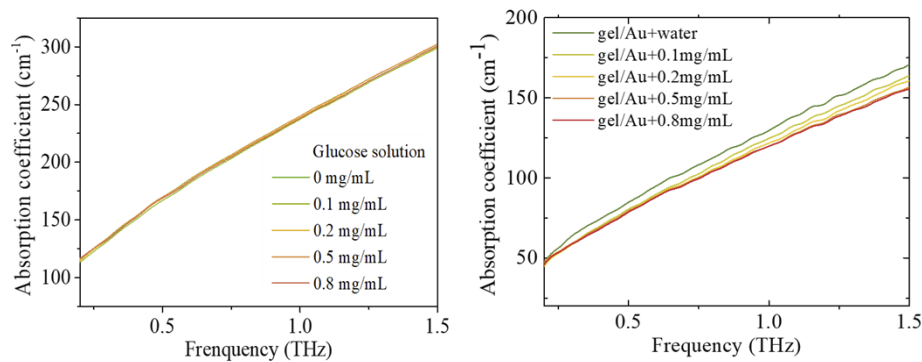

Fig. 3. (a) Broadband terahertz absorption coefficients measured in (a) different glucose solutions (0, 0.1, 0.2, 0.5, 0.8 mg/mL); (b) measured in the hydrogel platform with different glucose solutions.

The concentration-dependent change of THz absorption coefficients for the hydrogel samples averaged over 0.2 to 1.5 THz are plotted in Fig. 4. A nonlinear relationship can be clearly observed, which could be partly explained with adsorption dynamics. In an alkaline environment,

AuNPs in the hydrogel mainly existed in the form of $Au(OH)_{ad}$, in which $(OH)_{ad}$ stands for surface-adsorbed hydroxide species. Glucose molecules diffused into the hydrogel were first adsorbed on the surface of AuNPs, and then quickly oxidized to gluconolactone by $Au(OH)_{ad}$. As can be seen from the red curves in Fig. 4, the measured THz absorption of the hydrogel platform and the concentration of glucose can be well connected by the Langmuir-type of adsorption isotherm with a $R^2 = 0.9977$, while the Freundlich model results in a R^2 of 0.9874. The fitted parameters for both models are listed in Table 1. The glucose concentrations are fitted better with the Langmuir model than Freundlich, indicating that the majority of glucose molecules is adsorbed on homogeneous surface which corresponds well to the morphological features of AuNPs and ND surfaces (see Fig. 2 TEM images of ND@Au). The size of nanoparticle (both Au and ND) is much larger than that of the glucose molecule, making it a relatively homogeneous surface to the adsorption of glucose molecules. We presume that the same explanation can be applied to real blood samples, where the main interfering species are small molecules like glucose. Besides the adsorption dynamics, the environment pH may also contribute to the nonlinear relationship between $\Delta\alpha_{eff}$ and the glucose concentration. As the oxidation process proceeded, $Au(OH)_{ad}$ was reduced to $Au°$ and the gluconolactone accumulated in the hydrogel generating more H^+ ions which would lower the environment pH. The disruption of the alkaline environment would slow down the oxidation rate and eventually lead to a chemical equilibrium in the system.
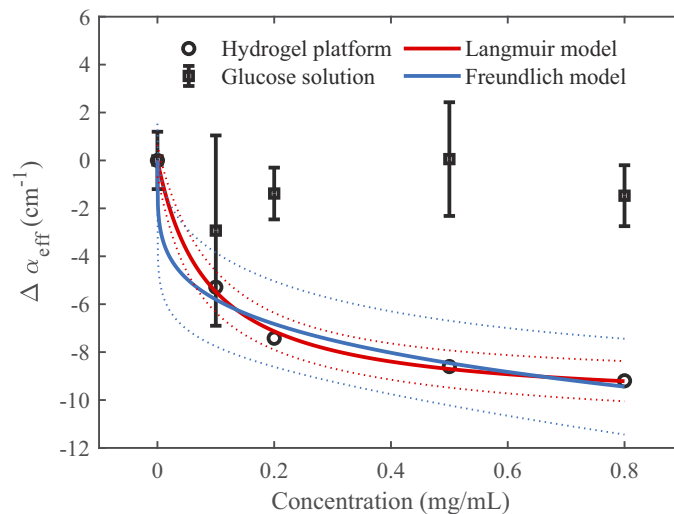

Fig. 4. The change of THz absorption coefficient for different glucose concentrations measured with our hydrogel platform. The results are fitted with the Langmuir and Freundlich isotherm models, respectively. The dashed lines represent the 95% confidence intervals of the models. For comparison, the change of THz absorption measured directly with glucose solutions are also shown in the figure.

Table 1. Parameters for Langmuir and Freundlich models.

Isotherm model	Langmuir			Freundlich		
Parameters	ϕ_{gmax}	K_L (mL/mg)	R^2	K_F (mL/mg)$^{1/n}$	n	R^2
	0.073	11.58	0.9977	0.071	0.234	0.9874

To account for the sensitivity of our sensing strategy, the LOD can be calculated following the S/N = 3 rule, where S is the signal and N is the noise. For our measurement protocol, N = 0.22

cm^{-1} which is the standard deviation for three separate measurements (Fig. S1). The LOD for the lowest detectable concentration is then determined to be 0.006 mg/mL (Fig. S2(a)) when assuming a Langmuir model with parameters shown in Table 1. However, since our sensor response is nonlinear, there exists a saturation point where further increasing of the glucose concentration is no longer detectable due to the saturated adsorption of glucose on nanoparticle surface. This saturation point can be determined by taking the derivative of the fitted Langmuir model, and finding the concentration where the derivative function is equal to 3N. As illustrated in Fig. S2 (b), the saturation point in our measurements is 1.06 mg/mL. According to the Food and Drug administration recommendations, glucose sensing devices are required to have an error < 20% in the range between 0.3mg/mL to 4 mg/mL. The upper detection limit is insufficient for our current fabricated hydrogel platform, due to the surface adsorption saturation. This can be improved with larger adsorption areas by either using smaller nanoparticles or applying techniques to inhibit the aggregation of nanoparticles.

3.3. *Effect of pH for sensitivity enhancement*

The results demonstrated above is a great improvement compared to the sensitivity provided by traditional THz-TDS measurements without the AuNP-embedded hydrogel platform [26,39]. One of the reasons is that the hydrogel platform greatly prohibited the absorption of bulk water: the absorption coefficient of the hydrogel samples at 1 THz is ~ 120 cm^{-1}, while that of bulk water and dilute glucose solutions is >200 cm^{-1} as shown in Fig. 3(b) and Fig. 3(a), respectively. As a result, the change induced by the different concentrations of glucose becomes more prominent. The other mechanism of the enhanced sensitivity could be attributed to the pH change in the solution as discussed in section 3.2. Glucose can be converted to gluconic acid in the presence of ND@Au in the alkaline condition, this reaction will eventually lead to a pH decrease in the system that will then result in the decreasing absorption of the terahertz waves [28].

To verify the above mechanism, freshly prepared AuNPs (25 mM) were added into the glucose solution with concentrations of 0.1, 1, 10, 50, and 100 mg/mL. However, as we mentioned above, subtle absorption changes induced by the pH are difficult to be probed in solution by THz-TDS measurements due to the strong absorption of H-bonded water network. It is also difficult to perform pH measurements directly in hydrogel samples. To overcome this issue, the prepared solutions were measured by THz-TDS reflection measurements on a well-studied metamaterial structure at various reaction times [40]. The change in reflection (ΔR) at the resonant frequency was calculated at the beginning, as well as after 1 and 15 min of reaction (see supplementary for more information). Figure 5(a)-(e) plot the ΔR vs. reaction time obtained for different glucose solutions with/without AuNPs. The change of pH values with reaction time was also recorded as illustrated in Fig. 5(f). Figure 5(a)-(e) clearly demonstrate that, with AuNPs in the solutions, THz reflection at the resonant frequency decreased to a lower value compared to those without AuNPs after 15 min. Moreover, the absolute change of reflection is greater for larger glucose concentrations as shown in Fig. 5(f). This result, as explained in Supplementary Fig.S3 [41], indicates that as the reaction proceeds, the solution becomes less absorbing. It has been reported that terahertz absorption declines with decreasing pH [28,42]. Therefore, it is verified that the pH drop induced by the oxidation reaction can indeed introduce an extra decrease in the absorption coefficient of the THz waves, which makes our ND@Au-embedded hydrogel platform more sensitive than traditional THz-TDS measurements performed on aqueous solutions [23,24].
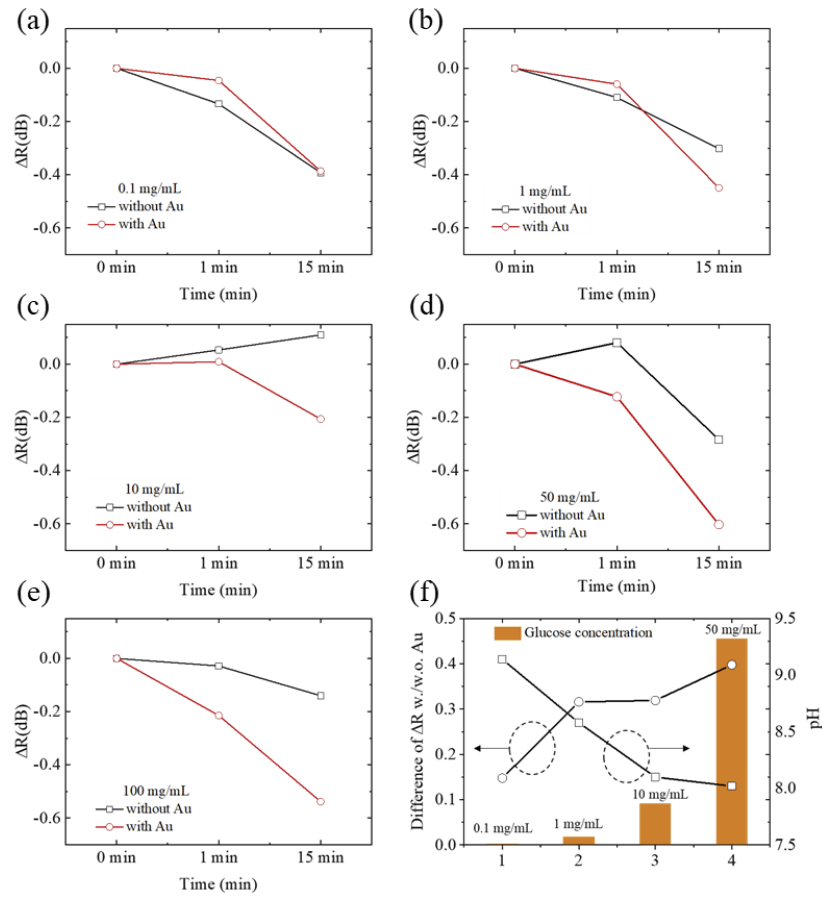
Fig. 5. (a-e) THz reflection at the metamaterial's resonant frequency obtained in different glucose solution with/without AuNPs. The glucose concentration was 0.1, 1, 10, 50, 100 mg/mL from (a) to (e), respectively. (f) pH after 15 min reaction time for different concentrations of glucose. The initial pH is pH = 10 adjusted by NaOH before reaction with glucose,

4. Conclusions

To conclude, we have designed an ND@Au-embedded hydrogel platform to enhance the sensitivity of glucose detection with terahertz frequencies. First of all, AuNPs were successfully synthesized on the surface of ND for the specific oxidation of glucose molecules. They were then evenly distributed in the hydrogel platform for glucose sensing. Finally, the hydrogel platform immersed with physiological concentrations of glucose solutions were measured with a THz-TDS system in transmission geometry. The absorption coefficient of the hydrogel sensing platform for glucose concentrations from 0 to 0.8 mg/mL can be clearly distinguished. The detectable concentration with our platform reaches physiological level, which is a great improvement compared to traditional THz-TDS measurements performed directly on aqueous glucose solutions. The relationship between the THz absorption of the sensing platform and the glucose concentration can be well described with the Langmuir isotherm model ($R^2 = 0.9977$). Besides the elimination of the bulk water absorption, we further verified that the enhanced detection sensitivity probably comes from the pH decrease induced by the oxidation of glucose in the presence of AuNPs.

We have provided a feasible strategy for glucose solution detection with terahertz spectroscopy. Our proposed non-enzymatic hydrogel detection platform is low cost, biocompatible and easy to fabricate. Challenges remain, such as how to control the total blood volume in hydrogel and how to control the initial environmental pH in the hydrogel. The above-mentioned issues may be solved by encapsulating the hydrogel in a confined space, and combining with other technologies to precisely control the injection volume. Many encapsulation technologies can be found in the literature, such as PDMS-based technologies. With properly designed electronics, circuits, and sensor enclosures, the proposed biosensor can be applied non-invasively for continuous glucose monitoring.

Disclosures. The authors declare no conflicts of interest.

Data availability. Data underlying the results presented in this paper are not publicly available at this moment but can be obtained upon reasonable request from the authors.

Supplemental document. See Supplement 1 for supporting content.

References

1. A. Sinclair, P. Saeedi, A. Kaundal, S. Karuranga, B. Malanda, and R. Williams, "Diabetes and global ageing among 65–99-year-old adults: Findings from the International Diabetes Federation Diabetes Atlas, 9th edition," Diabetes Res. Clin. Pract. **162**, 108078 (2020).
2. C. Espro, S. Marini, D. Giusi, C. Ampelli, and G. Neri, "Non-enzymatic screen printed sensor based on Cu_2O nanocubes for glucose determination in bio-fermentation processes," J. Electroanal. Chem. **873**, 114354 (2020).
3. Y. Yang, C. Yi, J. Luo, R. Liu, J. Liu, J. Jiang, and X. Liu, "Glucose sensors based on electrodeposition of molecularly imprinted polymeric micelles: A novel strategy for MIP sensors," Biosens. Bioelectron. **26**(5), 2607–2612 (2011).
4. A. Salim and S. Lim, "Recent advances in noninvasive flexible and wearable wireless biosensors," Biosens. Bioelectron. **141**(June), 111422 (2019).
5. G. Liu, J. Zhao, L. Qin, S. Liu, Q. Zhang, and J. Li, "Synthesis of an ordered nanoporous Cu/Ni/Au film for sensitive non-enzymatic glucose sensing," RSC Adv. **10**(22), 12883–12890 (2020).
6. Y. Dilmac and M. Guler, "Fabrication of non-enzymatic glucose sensor dependent upon Au nanoparticles deposited on carboxylated graphene oxide," J. Electroanal. Chem. **864**, 114091 (2020).
7. M. Adeel, M. M. Rahman, I. Caligiuri, V. Canzonieri, F. Rizzolio, and S. Daniele, "Recent advances of electrochemical and optical enzyme-free glucose sensors operating at physiological conditions," Biosens. Bioelectron. **165**(May), 112331 (2020).
8. M. Chen, X. Cao, K. Chang, H. Xiang, and R. Wang, "A novel electrochemical non-enzymatic glucose sensor based on Au nanoparticle-modified indium tin oxide electrode and boronate affinity," Electrochim. Acta **368**, 137603 (2021).
9. T. Zhang, J. Ran, C. Ma, and B. Yang, "A universal approach to enhance glucose biosensor performance by building blocks of Au nanoparticles," Adv. Mater. Interfaces **7**(12), 2000227 (2020).
10. L. Lin, S. Weng, Y. Zheng, X. Liu, S. Ying, F. Chen, and D. You, "Bimetallic PtAu alloy nanomaterials for nonenzymatic selective glucose sensing at low potential," J. Electroanal. Chem. **865**, 114147 (2020).
11. N. Lindner, A. Kuwabara, and T. Holt, "Non-invasive and minimally invasive glucose monitoring devices: a systematic review and meta-analysis on diagnostic accuracy of hypoglycaemia detection," Syst. Rev. **10**(1), 145 (2021).
12. H. Chen, Q. Shi, G. Deng, X. Chen, Y. Yang, W. Lan, Y. Hu, L. Zhang, L. Xu, C. Li, C. Zhou, Y. She, and H. Fu, "Rapid and highly sensitive colorimetric biosensor for the detection of glucose and hydrogen peroxide based on nanoporphyrin combined with bromine as a peroxidase-like catalyst," Sensors Actuators B Chem. **343**, 130104 (2021).
13. S. Delbeck, T. Vahlsing, S. Leonhardt, G. Steiner, and H. M. Heise, "Non-invasive monitoring of blood glucose using optical methods for skin spectroscopy-opportunities and recent advances," Anal. Bioanal. Chem. **411**(1), 63–77 (2019).
14. S. Haxha and J. Jhoja, "Optical based noninvasive glucose monitoring sensor prototype," IEEE Photonics J. **8**(6), 1–11 (2016).
15. N. V. Fredeen, N. I. Lesack, A. Ciocoiu, A. M. Garner, W. F. Zandberg, A. Jirasek, and J. F. Holzman, "The dynamic morphology of glucose as expressed via Raman and terahertz spectroscopy," OSA Contin. **3**(3), 515 (2020).
16. C. Zong, M. Wang, B. Li, X. Liu, W. Zhao, Q. Zhang, A. Liang, and Y. Yu, "Sensing of hydrogen peroxide and glucose in human serum: Via quenching fluorescence of biomolecule-stabilized Au nanoclusters assisted by the Fenton reaction," RSC Adv. **7**(43), 26559–26565 (2017).

17. J. Sawayama, T. Okitsu, A. Nakamata, Y. Kawahara, and S. Takeuchi, "Hydrogel glucose sensor with in vivo stable fluorescence intensity relying on antioxidant enzymes for continuous glucose monitoring," iScience **23**(6), 101243 (2020).

18. K. V. Larin, T. V. Ashitkov, M. Motamedi, and R. O. Esenaliev, "Specificity of noninvasive blood glucose monitoring with optical coherence tomography," Opt. Diagnostics Sens. Biomed. III **4965**, 25 (2003).

19. R. Zhang, S. Liu, H. Jin, Y. Luo, Z. Zheng, F. Gao, and Y. Zheng, "Noninvasive electromagneticwave sensing of glucose," Sensors **19**(5), 1151 (2019).

20. J. Dong, Q. Tao, M. Guo, T. Yan, and W. Qian, "Glucose-responsive multifunctional acupuncture needle: a universal SERS detection strategy of small biomolecules in vivo," Anal. Methods **4**(11), 3879–3883 (2012).

21. P. W. Barone, R. S. Parker, and M. S. Strano, "In vivo fluorescence detection of glucose using a single-walled carbon nanotube optical sensor: design, fluorophore properties, advantages, and disadvantages," Anal. Chem. **77**(23), 7556–7562 (2005).

22. N. Vieweg, F. Rettich, A. Deninger, H. Roehle, R. Dietz, T. Göbel, and M. Schell, "Terahertz-time domain spectrometer with 90 dB peak dynamic range," J. Infrared, Millimeter, Terahertz Waves **35**(10), 823–832 (2014).

23. V. P. Wallace, A. J. Fitzgerald, S. Shankar, N. Flanagan, R. Pye, J. Cluff, and D. D. Arnone, "Terahertz pulsed imaging of basal cell carcinoma ex vivo and in vivo," Br. J. Dermatol. **151**(2), 424–432 (2004).

24. J. Yang, L. Qi, B. Li, L. Wu, D. Shi, J. Ahmed Uqaili, and X. Tao, "A terahertz metamaterial sensor used for distinguishing glucose concentration," Results Phys. **26**(May), 104332 (2021).

25. J. Zhou, X. Zhao, G. Huang, X. Yang, Y. Zhang, X. Zhan, H. Tian, Y. Xiong, Y. Wang, and W. Fu, "Molecule-specific terahertz biosensors based on an aptamer hydrogel-functionalized metamaterial for sensitive assays in aqueous environments," ACS Sens. **6**(5), 1884–1890 (2021).

26. J. Zhou, X. Wang, Y. Wang, G. Huang, X. Yang, Y. Zhang, Y. Xiong, L. Liu, X. Zhao, and W. Fu, "A novel THz molecule-selective sensing strategy in aqueous environments: THz-ATR spectroscopy integrated with a smart hydrogel," Talanta **228**, 122213 (2021).

27. F. Sebastiani, C. Y. Ma, S. Funke, A. Bäumer, D. Decka, C. Hoberg, A. Esser, H. Forbert, G. Schwaab, D. Marx, and M. Havenith, "probing local electrostatics of glycine in aqueous solution by THz spectroscopy," Angew. Chem. Int. Ed. **60**(7), 3768–3772 (2021).

28. Z. Zang, S. Yan, X. Han, D. Wei, H. L. Cui, and C. Du, "Temperature- and pH-dependent protein conformational changes investigated by terahertz dielectric spectroscopy," Infrared Phys. Technol. **98**(March), 260–265 (2019).

29. J. Bastos-Arrieta, J. Muñoz, A. Stenbock-Fermor, D. N. Muraviev, F. Céspedes, L. A. Tsarkova, and M. Baeza, "Intermatrix Synthesis as a rapid, inexpensive and reproducible methodology for the in situ functionalization of nanostructured surfaces with quantum dots," Appl. Surf. Sci. **368**, 417–426 (2016).

30. A. Taketoshi, S. Takenouchi, T. Takei, and M. Haruta, "Synergetic combination of an enzyme and gold catalysts for glucose oxidation in neutral aqueous solution," Appl. Catal. A Gen. **468**, 453–458 (2013).

31. M. Dautta, M. Alshetaiwi, J. Escobar, and P. Tseng, "Passive and wireless, implantable glucose sensing with phenylboronic acid hydrogel-interlayer RF resonators," Biosens. Bioelectron. **151**(112004) (2020).

32. A. Al-Ibadi, J. Bou Sleiman, Q. Cassar, G. Macgrogan, H. Balacey, T. Zimmer, P. Mounaix, and J. P. Guillet, "Terahertz biomedical imaging: From multivariate analysis and detection to material parameter extraction," *Prog. Electromagn. Res. Symp.* 2756–2762 (2017).

33. D. Timothy D, R. G. Baraniuk, and D. M. Mittleman, "Material parameter estimation with terahertz time-domain spectroscopy," J. Opt. Soc. Am. A **18**(7), 1562–1571 (2001).

34. D. Lionel, F. Garet, and J. L. Coutaz, "Highly precise determination of optical constants and sample thickness in terahertz time-domain spectroscopy," Appl. Opt. **38**(2), 409–415 (1999).

35. X. Yang, Y. Yuan, Z. Dai, F. Liu, and J. Huang, "Optical property and adsorption isotherm models of glucose sensitive membrane based on prism SPR sensor," Sensors Actuators B Chem. **237**, 150–158 (2016).

36. N. Kim, M. Park, and D. Park, "A new efficient forest biowaste as biosorbent for removal of cationic heavy metals," Bioresour. Technol. **175**, 629–632 (2015).

37. H. Nguyen, S. You, and A. Hosseini-bandegharaei, "Mistakes and inconsistencies regarding adsorption of contaminants from aqueous solutions : A critical review," Water Res. **120**, 88–116 (2017).

38. J. Zhao, S. Lu, S. Fan, and Z. Qian, "Enhanced THz signal via Au encapsulated in hydrogel gel for non-enzymatic glucose sensing," Int. Conf. Infrared, Millimeter, Terahertz Waves, IRMMW-THz 2021-August, pp. 1–2 (2021).

39. C. Song, W. H. Fan, L. Ding, X. Chen, Z. Y. Chen, and K. Wang, "Terahertz and infrared characteristic absorption spectra of aqueous glucose and fructose solutions," Sci. Rep. **8**(1), 2–9 (2018).

40. P. Metamaterial, S. Wang, L. Xia, H. Mao, X. Jiang, S. Yan, H. Wang, D. Wei, H. Cui, and C. Du, "Terahertz biosensing based on a polarization-insensitive metamaterial,'," IEEE Photonics Technol. Lett. **28**(9), 1 (2016).

41. F. Miyamaru, K. Hattori, K. Shiraga, S. Kawashima, S. Suga, T. Nishida, M. W. Takeda, and Y. Ogawa, "Highly sensitive terahertz sensing of glycerol-water mixtures with metamaterials," J. Infrared, Millimeter, Terahertz Waves **35**(2), 198–207 (2014).

42. H.-Y. Huang, B. Su, S. Y. Shao, G. Y. Wang, and C. L. Zhang, "Terahertz absorption characteristics of solutions at different pH values," Infrared Millimeter-Wave, and Terahertz Technologies VII **11559**, 41 (2020).